

Hubble Space Telescope Detection of the Nucleus of Comet C/2014 UN₂₇₁ (Bernardinelli-Bernstein)

MAN-TO HUI (許文韜),¹ DAVID JEWITT,² LIANG-LIANG YU,¹ AND MAX J. MUTCHLER³

¹State Key Laboratory of Lunar and Planetary Science, Macau University of Science and Technology, Avenida Wai Long, Taipa, Macau

²Department of Earth, Planetary and Space Sciences, UCLA, 595 Charles Young Drive East, Los Angeles, CA 90095-1567, USA

³Space Telescope Science Institute, Baltimore, 3700 San Martin Drive, Baltimore, MD 21218, USA

(Received 2022; Revised March 1, 2022; Accepted 2022)

ABSTRACT

We present a high-resolution observation of distant comet C/2014 UN₂₇₁ (Bernardinelli-Bernstein) using the *Hubble Space Telescope* on 2022 January 8. The signal of the nucleus was successfully isolated by means of the nucleus extraction technique, with an apparent *V*-band magnitude measured to be 21.64 ± 0.11 , corresponding to an absolute magnitude of 8.62 ± 0.11 . The product of the visual geometric albedo with the effective radius squared is $p_V R_n^2 = 159 \pm 16 \text{ km}^2$. If the ALMA observation by Lellouch et al. (2022) refers to a bare nucleus, we derive a visual geometric albedo of 0.034 ± 0.008 and an effective diameter of $137 \pm 15 \text{ km}$. If dust contamination of the ALMA signal is present at the maximum allowed level (24%), we find nucleus diameter $119 \pm 13 \text{ km}$ and albedo of 0.044 ± 0.011 . In either case, we confirm that C/2014 UN₂₇₁ is the largest long-period comet ever detected. Judging from the measured surface brightness profile of the coma, whose logarithmic gradient varies azimuthally between ~ 1 and 1.7 in consequence of solar radiation pressure, the mass production is consistent with steady-state production but not with impulsive ejection, as would be produced by an outburst. Using aperture photometry we estimated an enormous (albeit uncertain) mass-loss rate of $\sim 10^3 \text{ kg s}^{-1}$ at a heliocentric distance of $\sim 20 \text{ au}$.

Keywords: comets: individual (C/2014 UN₂₇₁) — methods: data analysis

1. INTRODUCTION

Long-period comets are conceived to be compositionally some of the most pristine leftovers from the early solar system. For most of their lifetime, they have been stored in the low-temperature environment of the Oort cloud, at the edge of the solar system (Oort 1950). Recent years witnessed identifications of several long-period comets active at ultra-large heliocentric distances ($r_H \gtrsim 20 \text{ au}$), implying that the long-period comets may be more thermally processed than previously thought (Jewitt et al. 2017, 2021; Meech et al. 2017; Hui et al. 2018, 2019; Bernardinelli et al. 2021). Unlike most comets that are only active within the orbit of Jupiter ($r_H \lesssim 5 \text{ au}$) driven by sublimation of water ice (e.g., Whipple 1950), the cause of activity in distant comets remains unclear. Possible explanations for trans-Jovian

activity include sublimation of supervolatiles such as CO and CO₂ (e.g., Womack et al. 2017), crystallisation of amorphous ice (e.g., 1P/Halley; Prialnik & Bar-Nun 1992), and thermal memory from earlier perihelion passage (e.g., Comet Hale-Bopp; Szabó et al. 2008). Before we can use distantly active comets to directly investigate formation conditions of the early solar system, it is of great scientific importance to understand how their activity unfolds at great heliocentric distances.

The recent discovery of C/2014 UN₂₇₁ (Bernardinelli-Bernstein) offers us another excellent opportunity to study the distant population of comets. This long-period comet was found in Dark Energy Survey (DES) data at a remarkable inbound heliocentric distance of $r_H \approx 29 \text{ au}$, with additional predisccovery observations from $>30 \text{ au}$ from the Sun and exhibiting an obvious cometary feature at $r_H \gtrsim 20 \text{ au}$ (Bernardinelli et al. 2021; Farnham et al. 2021; Kokotanekova et al. 2021). According to the orbital solution by JPL Horizons, the current barycentric orbit of C/2014 UN₂₇₁ is highly el-

litical (eccentricity $e = 0.9993$) with a high perihelion distance of $q = 11.0$ au and a semimajor axis of $a = (1.6 \pm 0.2) \times 10^4$ au. Amongst many parameters, the size and the albedo of the cometary nucleus are often of the most importance. Recently, Lellouch et al. (2022) reported that the nucleus of the comet, 137 ± 17 km in diameter, is the largest amongst all known long-period comets, and has a visual geometric albedo $p_V = 0.049 \pm 0.011$. In this paper, we present our independent study of the nucleus size and albedo of the comet based an observation at a heliocentric distance of ~ 20 au, detailed in Section 2. We present our analysis in Section 3 and discussion in Section 4.

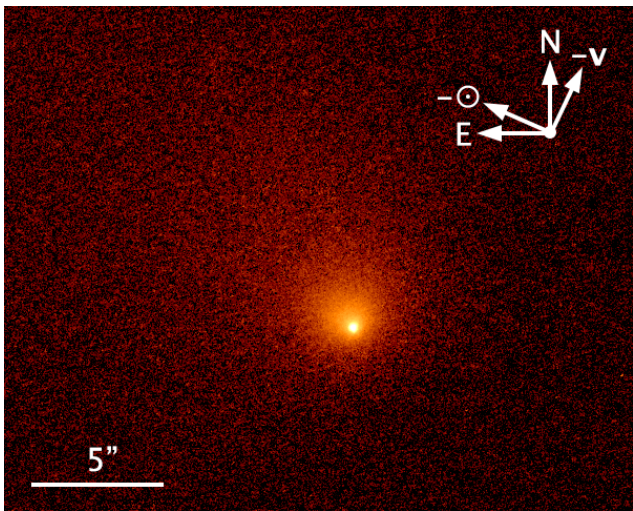


Figure 1. *HST*/WFC3 F350LP image of comet C/2014 UN₂₇₁ (Bernardinelli-Bernstein) median combined from the five individual exposures taken on 2022 January 8. The displayed image is scaled logarithmically and is oriented such that the J2000 equatorial north is up and east is left. Also marked are the directions of the projected antisolar vector ($-\odot$) and the projected negative heliocentric velocity of the comet ($-\mathbf{v}$). A scale bar of $5''$ in length is shown.

2. OBSERVATION

We secured five consecutive images each of 285 s duration in one visit of the comet under General Observer program 16886 using the 2.4 m *Hubble Space Telescope* (*HST*) and the UVIS channel of the Wide-Field Camera 3 (WFC3) on 2022 January 8. In order to achieve the maximal sensitivity of the facility, we exploited the F350LP filter, which has a peak system throughput of 29%, an effective wavelength of 585 nm, and a full-width at half maximum (FWHM) of 476 nm. For efficiency we read out only the UVIS2-2K2C-SUB aperture, the

2047×2050 full quadrant subarray on the UVIS channel with an image scale of $0''.04 \text{ pixel}^{-1}$ covering a field of view of $81'' \times 81''$ across. The telescope followed the nonsidereal motion of the comet, resulting in parallax-trailed background sources, despite the great distance of the comet. Image dithering was performed once between the third and fourth exposures so as to mitigate potential impacts from CCD artefacts. The observing geometry of the comet is summarised in Table 1.

In the *HST* images, the comet possesses a well-defined optocenter inside its bright quasircular coma of $\sim 4''$ in diameter, with a broad tail of $\gtrsim 15''$ in length directed approximately northeastwards (Figure 1).

3. ANALYSIS

In this section, we present our photometry to constrain the nucleus of comet C/2014 UN₂₇₁ based on our *HST* observation. Before carrying out any photometric analysis, we removed cosmic ray hits and hot pixels with the Laplacian cosmic ray rejection algorithm L.A. Cosmic by van Dokkum (2001) in IRAF (Tody 1986), which successfully rendered us with much cleaner images of the comet while its signal was left untouched.

3.1. Direct Photometry

The presence of the bright coma is obviously an obstacle to directly measuring the signal from the nucleus of the comet. However, this enabled us to place upper limits to the contribution of the nucleus.

The first method we applied was to place a circular aperture of $0''.20$ (5 pixels) in radius at the centroid of the comet in each of the five individual exposures, regard the measured signal as being all from the nucleus, and determine the sky background using a concentric annulus having inner and outer radii of $8''$ and $40''$, respectively, where contamination from the dust environment of the comet is completely negligible. We thereby obtained the apparent V -band magnitude of the region enclosed by the $0''.20$ radius aperture to be $m_V = 21.10 \pm 0.03$, in which the reported uncertainty is the standard deviation on the repeated measurements. Since the measured signal has contributions from both the nucleus and the surrounding coma enclosed by the aperture, the apparent magnitude of the nucleus must be fainter than the measured one. To correct for the observing geometry, we simply assumed a linear phase function with a slope of $\beta_\alpha = 0.04 \pm 0.02 \text{ mag deg}^{-1}$ appropriate for comets at small phase angles (e.g., Lamy et al. 2004). The result is highly unlikely to be altered greatly by the actual phase function, which is observationally unconstrained, in that the phase angle of the comet during our *HST* observation was merely $2^\circ.8$. Accordingly we estimate an

Table 1. Observing Geometry of Comet C/2014 UN₂₇₁ (Bernardinelli-Bernstein)

Date & Time (UT) ^a	Filter	t_{exp} (s) ^b	r_{H} (au) ^c	Δ (au) ^d	α (°) ^e	ε (°) ^f	$\theta_{-\odot}$ (°) ^g	$\theta_{-\mathbf{v}}$ (°) ^h	ψ (°) ⁱ
2022 Jan 08 09:24-09:56	F350LP	285	19.446	19.612	2.8	78.8	66.5	334.3	2.8

^aMid-exposure epoch.

^bIndividual exposure time.

^cHeliocentric distance.

^dComet-*HST* distance.

^ePhase angle (Sun-comet-*HST*).

^fSolar elongation (Sun-*HST*-comet).

^gPosition angle of projected antisolar direction.

^hPosition angle of projected negative heliocentric velocity of the comet.

ⁱOrbital plane angle (between *HST* and orbital plane of the comet).

uncertainty of $\sim \pm 0.06$ introduced by the phase function.

We computed the absolute magnitude of the nucleus from

$$H_{\text{n},V} = m_{\text{n},V} - 5 \log(r_{\text{H}}\Delta) - \beta_{\alpha}\alpha, \quad (1)$$

where the subscript “n” denotes parameters for the nucleus, r_{H} and Δ are respectively the heliocentric and cometocentric distances expressed in au, and α is the phase angle in degree. Substituting, we found that the nucleus of the comet must have $H_{\text{n},V} > 8.08 \pm 0.03$, in which the uncertainty is the standard error. The geometric albedo and the radius of the nucleus are directly related to the absolute magnitude by

$$p_V R_{\text{n}}^2 = 10^{0.4(m_{\odot,V} - H_{\text{n},V})} r_{\oplus}^2, \quad (2)$$

where p_V is the geometric albedo in the V band, R_{n} is the nucleus radius, and $m_{\odot,V} = -26.76 \pm 0.03$ is the apparent V -band magnitude of the Sun at heliocentric distance $r_{\oplus} = 1$ au (Willmer 2018). Inserting numbers, we found $p_V R_{\text{n}}^2 \lesssim (2.6 \pm 0.1) \times 10^2 \text{ km}^2$. Unfortunately the nucleus size of the comet is subjected to the assumption of the geometric albedo. However, Lellouch et al. (2022) lately reported $p_V = 0.049 \pm 0.011$ and $R_{\text{n}} = 69 \pm 9$ km using their ALMA observation in combination with the optical measurements by Bernardinelli et al. (2021). If their assumption that the coma contamination was negligible in the ALMA data is valid (but see Section 4.1), the reported size of the nucleus will be trustworthy, because the thermal emission measures R_{n}^2 and almost has no dependency upon the albedo. Therefore, assuming the aspect angles are not too different between the ALMA and *HST* observations, we found an

upper limit to the geometric albedo of the nucleus to be $p_V < 0.055 \pm 0.014$, contingent on the nucleus size derived by Lellouch et al. (2022).

As the coma is apparently bright in the *HST* observation, the first method only provides a coarse upper limit to the albedo of comet C/2014 UN₂₇₁. Thus, we adopted the second method to better constrain the parameter, in which the contribution from the coma was partially corrected. We still applied the same circular aperture of $0''.20$ in radius at the centroid of the comet. However, the coma in the contiguous annular region up to $0''.28$ from the centroid was measured and treated as the background value to be subtracted from the central aperture. The resulting flux measured by the aperture is still an upper limit to the counterpart from the nucleus. This is because this method underestimates the surface brightness of the coma in the central aperture, but it nevertheless provides a better constraint than does the first method, in which no correction was attempted whatsoever. We found the resulting apparent V -band magnitude to be $m_V = 21.22 \pm 0.03$, corresponding to $H_{\text{n},V} > 8.20 \pm 0.03$, and $p_V < 0.050 \pm 0.012$, if still assuming the nucleus size reported by Lellouch et al. (2022). In comparison, Lellouch et al. (2022) reported the exact geometric albedo of the comet, rather than an upper limit, to be $p_V = 0.049 \pm 0.011$, which is indistinguishable from what we obtained from the second method. We refrain from the relevant discussion until in Section 4.

3.2. Nucleus Extraction

Given the ultrastable point-spread function (PSF) and the supreme spatial resolution and sensitivity of the

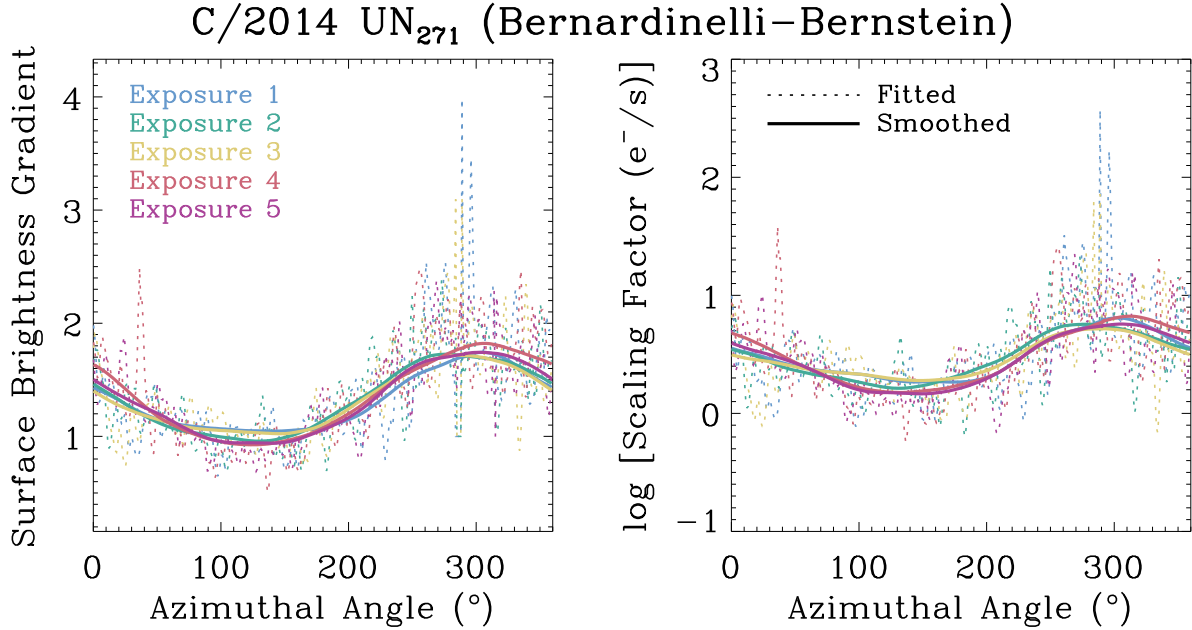


Figure 2. Best-fitted (dotted lines) and smoothed (solid lines) logarithmic surface brightness gradient and the scaling factor of the coma both as functions of the azimuthal angle. Results from different individual exposures are distinguished by colors, as indicated in the legend in the left panel. The surface brightness profile of the comet in annular regions between $0''.24$ and $0''.80$ from the optocenter in the individual exposures was used for the best fits.

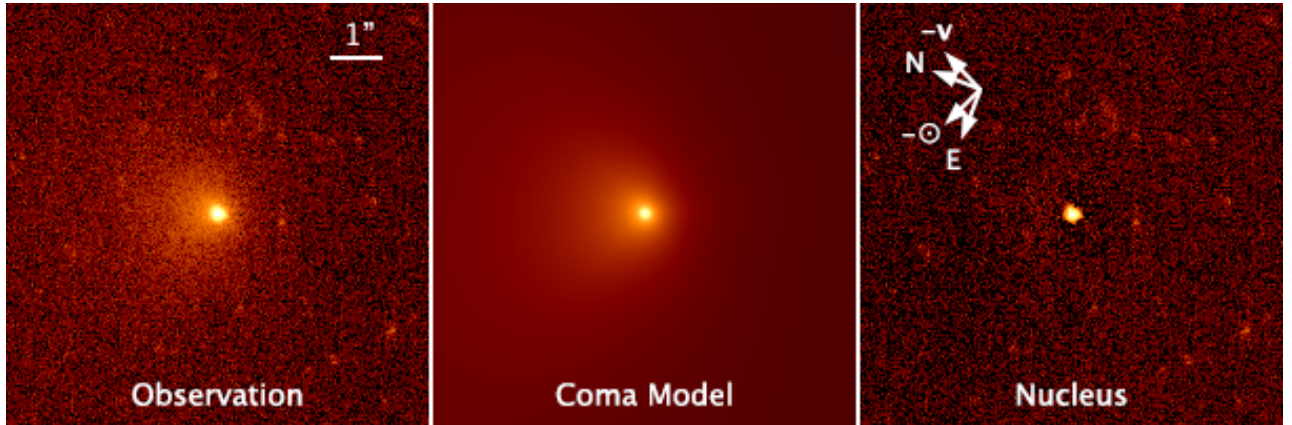


Figure 3. Brief illustration of how the nucleus extraction technique was applied for the second *HST*/WFC3 exposure as an example. The coma model (middle panel) was obtained by means of fitting the surface brightness profile of the observed image (left panel), followed by subtracting the former from the latter, unveiling a stellar source at the original centroid of the comet in the residual image (right panel), which we interpreted as the nucleus of comet C/2014 UN₂₇₁. A $1''$ scale bar and the cardinal directions, along with the directions of the projected antisolar vector and the projected negative heliocentric velocity of the comet are marked.

HST/WFC3 camera, we opted to employ the nucleus extraction technique, which has been successfully applied for a number of comets previously observed by *HST* (e.g., Lamy et al. 1998a,b, 2009, 2011) and systematically evaluated (Hui & Li 2018). The basic idea of the technique is to remove the contamination of the coma by means of fitting its surface brightness profile and extrapolating inwards to the near-nucleus region, assuming that the coma is optically thin, such that the

signal from the coma and that from the nucleus are separable. The surface brightness of the coma was fitted by an azimuthally dependent power-law model. We expressed the surface brightness of the comet as a function of the angular distance to the nucleus (ρ) and the az-

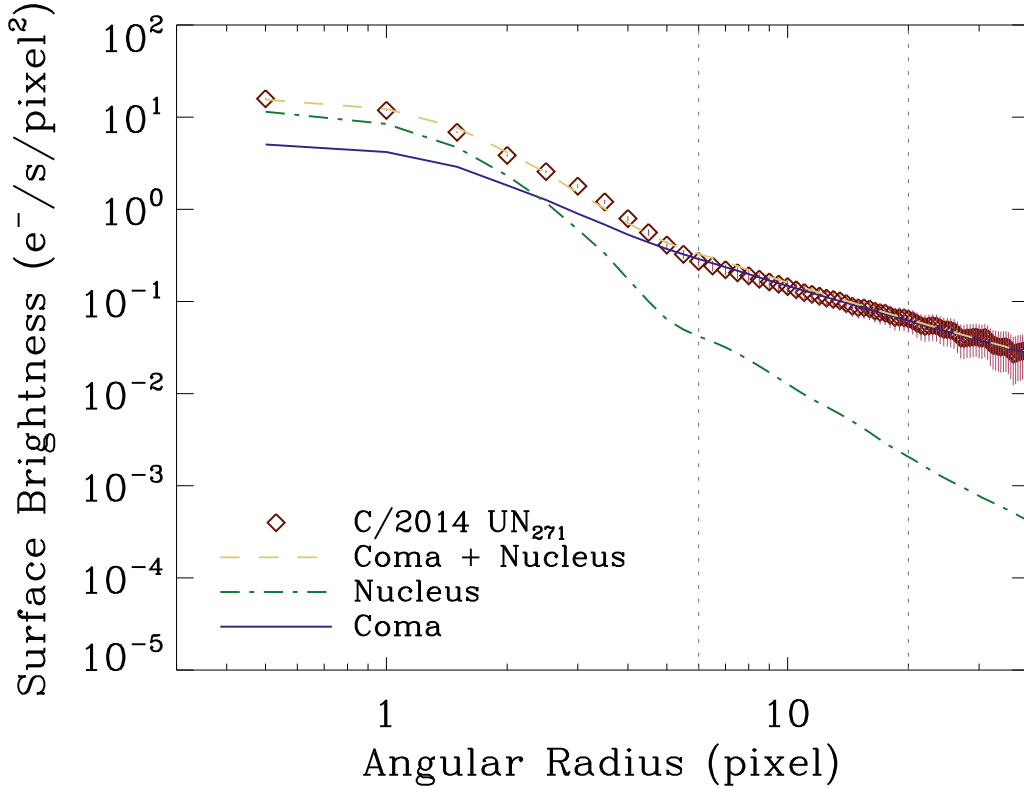


Figure 4. Radial profile comparison between the coma (violet solid line), the nucleus (green dashed-dotted line), and the total (yellow dashed line) models, and the observation (red diamonds with error bars given) plotted on a log-log scale for the second individual *HST* exposure as an example. Results from the other four exposures are visually similar and are therefore not displayed separately for brevity. The two grey vertical dotted lines mark the annular radius range (6-20 pixels, or $0''.24$ - $0''.80$) within which the surface brightness profile of the coma was fitted.

imuthal angle (θ) in the sky plane as

$$\begin{aligned} \Sigma_{\text{m}}(\rho, \theta) &= \left[k_{\text{n}} \delta(\rho) + k_{\text{c}}(\theta) \left(\frac{\rho}{\rho_0} \right)^{-\gamma(\theta)} \right] * \mathcal{P} \\ &= k_{\text{n}} \mathcal{P} + \left[k_{\text{c}}(\theta) \left(\frac{\rho}{\rho_0} \right)^{-\gamma(\theta)} \right] * \mathcal{P}. \end{aligned} \quad (3)$$

Here, k_{n} and k_{c} are the scaling factors for the nucleus and coma, respectively, δ is the Dirac delta function, γ is the logarithmic surface brightness gradient of the coma, \mathcal{P} is the normalised PSF kernel, $\rho_0 = 1$ pixel is a normalisation factor to guarantee that the two scaling factors share the same unit, and the symbol $*$ is the convolution operator.

We followed the procedures detailed in Hui & Li (2018) to extract the nucleus signal from our *HST* data. Basically, we fitted the surface brightness profile of the coma in azimuthal segments of 1° over some annular region where the contribution from the nucleus is negligible in the individual exposures. Smoothing of the best-fit parameters for the coma was carried out so as to

alleviate fluctuations due to uncleaned artefacts caused by cosmic ray hits (Figure 2), followed by extrapolating the surface brightness profile inwards to the near-nucleus region and convolution with the *HST*/WFC3 PSF model generated by TinyTim (Krist et al. 2011). Subtraction of the coma model from the observed image revealed a well-defined stellar source around the original centroid of the comet in the residual image, which was measured to have a FWHM of $0''.071 \pm 0''.004$ (or 1.8 ± 0.1 pixels), in line with the FWHM of the PSF model by TinyTim, therefore interpreted as the nucleus of the comet (Figure 3). We then fitted the PSF model to the source, whereby we obtained the scaling factor k_{n} as the total flux for the nucleus using aperture photometry. Comparisons between radial brightness profiles of the observation and the models are plotted in Figure 4.

To test the reliability of the results, we varied a number of parameters, including the subsampling factor, the fitted region, and the smoothed angle bins, only to find that the variation is always only $\lesssim 10\%$ of the measured flux, no greater than the standard deviation of the re-

peated measurements. Therefore, we used the latter as the uncertainty of the nucleus flux obtained from the nucleus extraction technique, although this most likely overestimates the actual error.

It is known that the nucleus extraction technique produces systematic biases in determination of nucleus signal that are difficult to correct, and that it can even fail on a few occasions (Hui & Li 2018). In order to ascertain how our result might be biased by the technique, we assessed the ratio between the nucleus flux and the total flux measured with a $0''.60$ radius circular aperture, which was found to be always $\gtrsim 30\%$, falling into a regime where the bias is totally negligible (Hui & Li 2018). Therefore, we are confident that the signal of the nucleus determined from our *HST* observation on comet C/2014 UN₂₇₁ is robust.

The result is that we found the apparent *V*-band magnitude of the nucleus to be $m_{n,V} = 21.64 \pm 0.11$. Substitution into Equation (1) yields $H_{n,V} = 8.62 \pm 0.11$, which is clearly fainter than what Bernardinelli et al. (2021) reported based on their optical observations ($H_{n,V} = 8.21 \pm 0.05$, converted from the Sloan bands; Lellouch et al. 2022), and corresponds to $p_V R_n^2 = (1.59 \pm 0.16) \times 10^2 \text{ km}^2$ yielded by Equation (2). Still adopting the nucleus size reported by Lellouch et al. (2022), we determine a nucleus geometric albedo of $p_V = 0.034 \pm 0.009$, in which the uncertainty was properly propagated from all measured and reported errors. Our result suggests a lower albedo for the nucleus surface, because it is possible that the photometry by Bernardinelli et al. (2021) is contaminated by the dust environment of comet C/2014 UN₂₇₁. Nonetheless, the albedo we derived is unremarkable in comparison to those of other cometary nuclei (distributed in a narrow range of $p_V \approx 0.02\text{-}0.06$; Lamy et al. 2004).

4. DISCUSSIONS

4.1. Nucleus Size

Our analysis of the *HST* observation of comet C/2014 UN₂₇₁ provided us with an estimate of its nucleus absolute magnitude ~ 0.41 mag fainter than the result by Bernardinelli et al. (2021), presumably as a result of coma contamination in the large aperture optical photometry used by these authors. If there is no dust contamination of the 233 GHz ALMA signal, the nucleus albedo must be lower than the one derived by Lellouch et al. (2022), as shown by the hollow green and filled blue circles in Figure 5.

However, Lellouch et al. (2022) concluded that up to $\sim 24\%$ of the 233 GHz continuum flux could be from an unseen dust coma in their data. In this case, we estimate that the effective diameter of the comet would

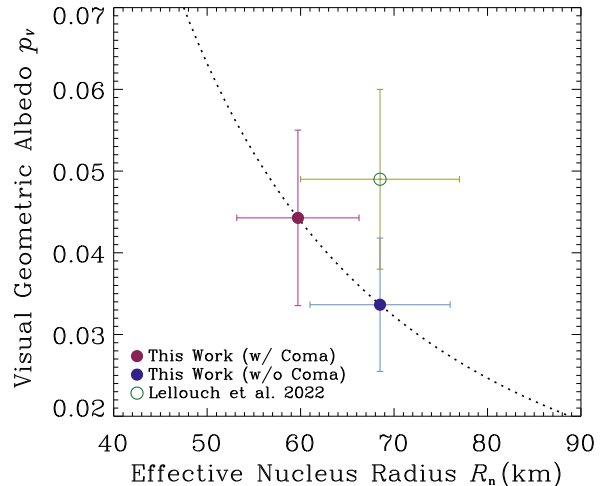


Figure 5. Geometric albedo vs. effective radius of the nucleus of C/2014 UN₂₇₁. The dotted line shows $p_V R_n^2 = 159 \text{ km}^2$, as found from our *HST* photometry. The nucleus parameters must fall on this line. The hollow green circle marks the measurement by Lellouch et al. (2022), which relies upon large-aperture (more likely coma-contaminated) photometry of the nucleus by Bernardinelli et al. (2021). The filled blue and purple circles show two solutions using the new $p_V R_n^2$ constraint both with and without the $\sim 24\%$ dust contamination of the 230 GHz thermal signal allowed by Lellouch et al. (2022).

be reduced to $119 \pm 15 \text{ km}$ and the geometric albedo increased to $p_V = 0.044 \pm 0.012$, shown as a filled purple circle in Figure 5. In order to affect the 233 GHz cross-section, dust in the comet would need to be large. Two observations suggest that the coma might indeed be rich in large grains. Firstly, independent observations of other long-period comets (notably C/2017 K2; (e.g., Jewitt et al. 2017; Hui et al. 2018; Jewitt et al. 2019a)) have convincingly revealed that submillimeter and larger dust grains are produced at great heliocentric distances. Secondly, based on a syndyne-synchrone computation, Farnham et al. (2021) deduced that C/2014 UN₂₇₁ has been ejecting submillimeter sized and larger dust grains for years prior to the epoch of observation. The driver of mass loss at distances $\sim 20 \text{ au}$ (and potentially at much larger distances; Bouziani & Jewitt (2022)) is presumably the sublimation of carbon monoxide.

An additional factor which might affect estimates of the albedo is the rotation of the nucleus, resulting in cross-sections different between the ALMA and *HST* observations. However, most known cometary nuclei have aspect ratios $\lesssim 2:1$ (e.g., Lamy et al. 2004) and so we do not expect rotational effects in nucleus photometry larger than a factor of two.

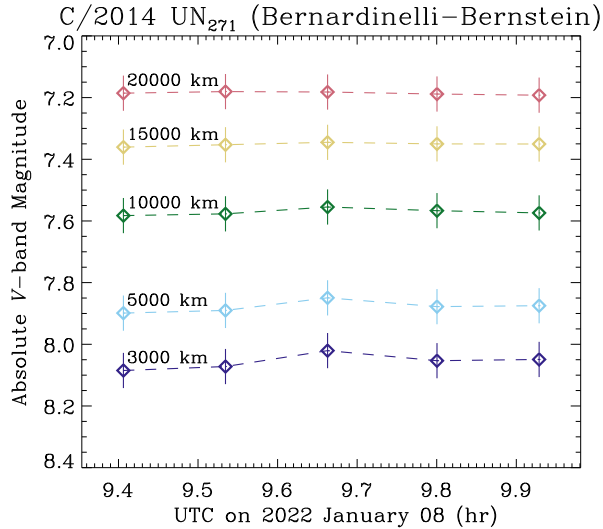


Figure 6. Absolute V-band magnitude as a function of time in UTC on 2022 January 8 for each of the fixed linear apertures, distinguished by colors. The radii of the apertures are explicitly labelled on the plot. The reported errors are dominated by the uncertainty in the assumed phase function.

In short, our improved estimate of the absolute magnitude shows that the nucleus of C/2014 UN₂₇₁ is slightly smaller or slightly darker than found by Lellouch et al. (2022) but we strongly confirm their result that the nucleus is larger than any other previously measured long-period cometary nucleus. Figure 5 is shown as a comparison of the results.

4.2. Mass Loss

We measured the logarithmic surface brightness gradient of the coma in Section 3.2, which allows for qualitative diagnosis of the observed activity. In steady state, the surface brightness gradient of the coma is expected to be $\gamma = 1$ but will be steepened to ~ 1.5 by the solar radiation pressure (Jewitt & Meech 1987). Indeed, we found that the surface brightness gradient of the coma lies within a range between ~ 1 and 1.7 (see Figure 2), consistent with the coma produced in steady state. The result that the gradient is generally steeper around the azimuthal angles facing towards the Sun and is shallower otherwise is expected.

In addition to characterising the properties of the nucleus of comet C/2014 UN₂₇₁, we also performed photometry of the comet in multiple fixed linear circular apertures aiming to measure its coma. The background was determined in the same fashion as in the first method in Section 3.1. For correction of the observing geometry, we still assumed a linear phase function with slope $\beta_\alpha = 0.04 \pm 0.02$ mag deg⁻¹, which is also ap-

propriate for cometary dust at small phase angles (e.g., Kolokolova et al. 2004, and citations therein). We plot the measurements in Figure 6, in which the errors are primarily attributed to the uncertainty in the assumed phase function.

In the following we estimate the mass loss of the comet using the largest fixed linear aperture in the order-of-magnitude manner. Presuming that the total cross-section of the dust particles having mean radius $\bar{a}_d \sim 0.1$ mm was ejected in steady state at speeds $v_{ej} \sim 10$ m s⁻¹ (Farnham et al. 2021), we can then relate the mass-loss rate to the measured absolute magnitude of the dust by

$$\bar{M}_d \sim \frac{\pi \rho_d \bar{a}_d v_{ej} r_\oplus^2}{\ell p_V} 10^{0.4(m_{\odot,V} - H_{d,V})}, \quad (4)$$

in which the subscript “d” denotes parameters of the dust grains, $\rho_d \sim 1$ g cm⁻³ is the nominal bulk density of the dust grains, and $\ell = 2 \times 10^4$ km is the projected radius of the largest aperture we used to measure the coma. By substitution, we find the dust mass-loss rate $\bar{M}_d \sim 10^3$ kg s⁻¹. In comparison, distant comet C/2017 K2 (PANSTARRS) was estimated to exhibit a dust mass-loss rate of $\sim 10^2$ kg s⁻¹ at $r_H \lesssim 20$ au (Jewitt et al. 2017; Hui et al. 2018; Jewitt et al. 2021), while Szabó et al. (2008) reported $\sim 10^3$ kg s⁻¹ for comet Hale-Bopp at similar heliocentric distances on the outbound leg of its orbit. Yet none of the aforementioned values are better than order-of-magnitude estimates.

5. SUMMARY

We employed the *Hubble Space Telescope* to observe the distant active comet C/2014 UN₂₇₁ (Bernardinelli-Bernstein) on 2022 January 8. The key conclusions are:

1. The apparent V-band magnitude of the bare cometary nucleus was measured using high resolution HST data and a profile fitting technique to be 21.64 ± 0.11 , corresponding to an absolute magnitude of 8.62 ± 0.11 . The nucleus must satisfy $p_V R_n^2 = (1.59 \pm 0.16) \times 10^2$ km², where p_V and R_n are the geometric albedo and effective nucleus radius, respectively.
2. Assuming that the ALMA photometry by Lellouch et al. (2022) is free from any contamination from the dust coma, we estimated the visual geometric albedo and the effective radius of the nucleus to be $p_V = 0.034 \pm 0.008$ and $R_n = 69 \pm 8$ km, respectively. If the maximal $\sim 24\%$ contamination of the ALMA flux contributed by coma is considered, we instead derive $p_V = 0.044 \pm 0.011$ and $R_n = 60 \pm 7$ km. The nucleus likely lies between these extremes.

3. The logarithmic surface brightness gradient of the coma varies between $\gamma \sim 1$ and 1.7 depending on the azimuthal angle, indicating that the dust grains are ejected in a protracted rather than an impulsive manner.
4. From the photometric measurements of the coma, we estimated the dust mass-loss rate of the comet to be $\sim 10^3 \text{ kg s}^{-1}$ at heliocentric distance $r_H \sim 20 \text{ au}$.

Facilities: HST

Software: IDL, IRAF (Tody 1986), L.A. Cosmic (van Dokkum 2001), TinyTim (Krist et al. 2011)

1 This research is based on observations from program GO
2 16886 made with the NASA/ESA *Hubble Space Tele-*
3 *scope* obtained from the Space Telescope Science Insti-
4 tute, which is operated by the Association of Universities
5 for Research in Astronomy, Inc., under NASA contract
6 NAS 5–26555. MTH appreciates great support and en-
7 couragement from Kiwi.

REFERENCES

- Bernardinelli, P. H., Bernstein, G. M., Montet, B. T., et al. 2021, *ApJL*, 921, L37. doi:10.3847/2041-8213/ac32d3
- Bouziani, N. & Jewitt, D. 2022, *ApJ*, 924, 37. doi:10.3847/1538-4357/ac323b
- Farnham, T. L., Kelley, M. S. P., & Bauer, J. M. 2021, *PSJ*, 2, 236. doi:10.3847/PSJ/ac323d
- Fornasier, S., Lellouch, E., Müller, T., et al. 2013, *A&A*, 555, A15. doi:10.1051/0004-6361/201321329
- Gimeno, G., Roth, K., Chiboucas, K., et al. 2016, *Proc. SPIE*, 9908, 99082S. doi:10.1117/12.2233883
- Harris, A. W. 1998, *Icarus*, 131, 291. doi:10.1006/icar.1997.5865
- Hui, M.-T. & Li, J.-Y. 2018, *PASP*, 130, 104501. doi:10.1088/1538-3873/aad538
- Hui, M.-T., Jewitt, D., & Clark, D. 2018, *AJ*, 155, 25. doi:10.3847/1538-3881/aa9be1
- Hui, M.-T., Farnocchia, D., & Micheli, M. 2019, *AJ*, 157, 162. doi:10.3847/1538-3881/ab0e09
- Jewitt, D. C. & Meech, K. J. 1987, *ApJ*, 317, 992. doi:10.1086/165347
- Jewitt, D., Hui, M.-T., Mutchler, M., et al. 2017, *ApJL*, 847, L19. doi:10.3847/2041-8213/aa88b4
- Jewitt, D., Agarwal, J., Hui, M.-T., et al. 2019, *AJ*, 157, 65. doi:10.3847/1538-3881/aaf38c
- Jewitt, D., Kim, Y., Luu, J., et al. 2019, *AJ*, 157, 103. doi:10.3847/1538-3881/aafe05
- Jewitt, D., Kim, Y., Mutchler, M., et al. 2021, *AJ*, 161, 188. doi:10.3847/1538-3881/abe4cf
- Kelley, M. S. P., Lister, T., & Holt, C. E. 2021, *The Astronomer’s Telegram*, 14917
- Kokotanekova, R., Lister, T., Bannister, M., et al. 2021, *The Astronomer’s Telegram*, 14733
- Kokololova, L., Hanner, M. S., Lvasseur-Regourd, A.-C., et al. 2004, *Comets II*, 577
- Krist, J. E., Hook, R. N., & Stoehr, F. 2011, *Proc. SPIE*, 8127, 81270J. doi:10.1117/12.892762
- Lamy, P. L., Toth, I., Jorda, L., et al. 1998, *A&A*, 335, L25
- Lamy, P. L., Toth, I., & Weaver, H. A. 1998, *A&A*, 337, 945
- Lamy, P. L., Toth, I., Fernandez, Y. R., et al. 2004, *Comets II*, 223
- Lamy, P. L., Toth, I., Weaver, H. A., et al. 2009, *A&A*, 508, 1045. doi:10.1051/0004-6361/200811462
- Lamy, P. L., Toth, I., Weaver, H. A., et al. 2011, *MNRAS*, 412, 1573. doi:10.1111/j.1365-2966.2010.17934.x
- Lellouch, E., Moreno, R., Bockelée-Morvan, D., et al. 2022, arXiv:2201.13188
- Meech, K. J., Kleyna, J. T., Hainaut, O., et al. 2017, *ApJL*, 849, L8. doi:10.3847/2041-8213/aa921f
- Oort, J. H. 1950, *BAN*, 11, 91
- Prialnik, D. & Bar-Nun, A. 1992, *A&A*, 258, L9
- Ridden-Harper, R., Bannister, M. T., & Kokotanekova, R. 2021, *Research Notes of the American Astronomical Society*, 5, 161. doi:10.3847/2515-5172/ac1512
- Szabó, G. M., Kiss, L. L., & Sárneczky, K. 2008, *ApJL*, 677, L121. doi:10.1086/588095
- Szabó, G. M., Kiss, L. L., Pál, A., et al. 2012, *ApJ*, 761, 8. doi:10.1088/0004-637X/761/1/8
- Tody, D. 1986, *Proc. SPIE*, 627, 733. doi:10.1117/12.968154

van Dokkum, P. G. 2001, PASP, 113, 1420.

doi:10.1086/323894

Whipple, F. L. 1950, ApJ, 111, 375. doi:10.1086/145272

Willmer, C. N. A. 2018, ApJS, 236, 47.

doi:10.3847/1538-4365/aabfdf

Womack, M., Sarid, G., & Wierzos, K. 2017, PASP, 129,
031001. doi:10.1088/1538-3873/129/973/031001